Desalination and Water Treatment
www.deswater.com
doi: 10.1080/19443994.2015.1017321

57 (2016) 7131–7148
April

Taylor & Francis
Taylor & Francis Group

Closed circuit PRO series no 3: status and prospects for PRO hydroelectric power generation from sea–river water like salinity gradients

Avi Efraty

Osmotech Ltd, P.O. Box 132, Har Adar 90836, Israel, Tel. +972 52 4765 687; Fax: +972 2 570 0262; email: efraty.adt@012.net.il

Received 5 December 2013; Accepted 3 February 2015

ABSTRACT

The present status and future prospects of pressure related osmosis (PRO) for hydroelectric power generation from the most widespread salinity gradients of seawater and river water systems (SW–RW) are analyzed by a theoretical model in terms of the membrane, module, and method. The selected membrane in the model analysis comprises MP # 1 of the highest presently known permeability coefficient (5.81 Lmh/bar) with a projected peak power density of 10 W/m^2 at 13 bar. The performance of the referred MP # 1 membrane was ascertained in the context of the closed circuit PRO (CC-PRO) and conventional PRO methods at different HSF (high salinity feed or "draw" solution) to permeate flow ratio (δ), and percent permeate (α) in HSDF (high salinity diluted feed or diluted "draw" solution) with emphasis of the membrane power density (PD) and the net electric power density (NEPD) which takes into account the fraction of power consumed by the auxiliary pumps. The theoretical CC-PRO simulation of a typical SW–RW salinity gradient using MP # 1 with actual/ideal flux ratio (β) of 0.374 shows maximum membrane PD as function of flow ratio (δ) and hydraulic pressure difference in the declined order of 10.00 W/m^2 at 13 bar ($\delta > 40$); 8.52 W/m^2 at 12 bar ($\delta = 5.0$); 7.45 W/m^2 at 11 bar ($\delta = 2.5$); 6.13 W/m^2 at 10 bar ($\delta = 1.25$); 5.69 W/m^2 at 10 bar ($\delta = 1.00$); and 5.16 W/m^2 at 9 bar ($\delta = 0.75$). The simulated NEPD availability of this system reveals the declined order of 4.2 W/m^2 at 13 bar ($\delta = 2.5$) 4.1 W/m^2 at 12 bar ($\delta = 1.25$); 3.9 W/m^2 at 11 bar ($\delta = 1.00$); and 3.6 W/m^2 at 10 bar ($\delta = 0.75$). Compared with the CC-PRO technology of near absolute energy conversion efficiency, the PD and NEPD of the conventional PRO technique with MP # 1 show lower values since they depend on the efficiency of the energy recovery device. A further decline of PD and NEPD availability also takes place for membrane having $A < 5.81$ Lmh/bar and/or $\beta < 0.374$, suggesting the low feasibility of the SW–RW gradient systems for economic PRO hydroelectric power generation in the near future.

Keywords: Forward osmosis; Osmotic power; Salinity gradient power; Osmotic power generation; Pressure retarded osmosis (PRO); Closed circuit PRO; Osmotic gradient driven processes; Clean energy sources

1. Introduction

In light of the rapidly expanding global population, increased standards of living, rising energy consumption, and growing demand for polluting fossil fuels, the need to develop large-scale viable clean energy technologies for widespread applications worldwide is an issue of obvious environmental and economical importance. Conventional hydroelectric power

generation at present supplies some ~2.5% of the global power needs with other clean energy sources (e.g. wind, solar, biomass, geothermal, etc.) account for only ~0.5%. A newly emerging technology for large-scale clean energy generation is the so-called pressure retarded osmosis (PRO) conceived by Loeb [1,2] in 1975, the same person who 15 years earlier discovered [3] the application of reverse osmosis (RO) for seawater and brackish water desalination. PRO is a membrane-based technology [4,5] for hydroelectric power generation from salinity gradients of worldwide abundance such as rivers at their outlets to the sea or any other two sources of different concentrations. When two streams of different salinity meet on the opposite sides of a semipermeable membrane, pressurized water permeation takes place from the low to high concentration side of the semimembrane by a natural forward osmosis (FO) process and the created pressurized stream can be used for hydroelectric power generation as well as for other applications including desalination [6]. PRO power generation prospects depend on the magnitude of the salinity gradient as well as on the availability of suitable membranes and technology for such an application, aspects to be considered next.

1.1. Salinity gradient sources

Salinity gradient sources are the basic fuels for the PRO power generation technology with larger gradients concomitant with greater power output and vice versa. Although the awareness of the enormous osmotic pressure-difference (~250 bar) between the Dead-Sea (35%) and the Mediterranean-Sea (4.0%) contributed to the inception of PRO by Loeb [7], the major efforts today are directed toward the salinity gradient systems seawater and river water systems (SW–RW), SWB–RW and SWB–BW; where SW stands for seawater, SWB for seawater brine from SWRO desalination plants and BW for low salinity brackish water like sources including treated domestic effluents. The *Statkarft* company [8–10] in Norway pioneered the efforts to develop PRO commercial applications for SW–RW type salinity gradient systems; whereas the "*Mega-ton Water System Project*" [11–13] in Japan has been geared towards the development of commercial applications for the SWB–BW type salinity gradient systems with some promising results already received. Very little attention has been given thus far to salinity gradients comprising of SW and its concentrates found in evaporation ponds of hundreds of salt productions factories worldwide which could be used for PRO power generation apart from their traditional role.

1.2. Semipermeable PRO membranes for hydroelectric power generation

Semipermeable membranes for PRO applications should possess features such as a high permeability coefficient (A), a sufficiently low salt diffusion coefficient (B), small structural parameters (S), and a sufficiently high mechanical stability to withstand applied pressures of maximum power density. Power density of PRO membranes (W/m^2) is expressed by Eq. (1); wherein, J_w stands for ideal flux and p_a for applied hydraulic pressure. Ideal water flux is expressed by Eq. (2); however, the reverse salt diffusion flux (J_s) expressed by Eq. (3) as a result of the concentration difference between the high salinity draw (C_D) and low salinity feed (C_F) solutions could not be ignored. The membrane support layer which separates the bulk concentrations creates a unique zone of different stationary state conditions since the effective feed concentration at the active thin film composite (TFC) layer (C_{F-E}) is higher than that in the bulk ($C_{F-E} > C_F$) due to J_s and therefore, the effective osmotic pressure difference across the active membrane layer ($\Delta\pi_m$) is lower than that between the bulk solutions ($\Delta\pi_m < \Delta\pi$) and this will prompt a lower effective net driving pressure across the active layer ($\Delta\pi_m - p_a$) causing a lower PRO power output. The effects created in the support layer on PRO power generation, the so-called internal concentration polarization (ICP) effects, are function of A, B, and the structural parameter S defined by Eq. (4) as function of support's thickness (t_s), tortuosity (τ), and porosity (ε). The S parameter expresses the distance which a solute particle needs to pass from the active layer to the bulk of the feed solution. The detrimental effects on power availability of PRO membranes are well understood today in terms of ICP, external concentrations polarization (ECP) and structural parameters arising from the intrinsic characteristic features A, B, and S of membranes. In light of the aforementioned, the actual flux (J_{wa}) and power density (W_a) of PRO membranes can be expressed by Eqs. (5) and (6), respectively, using a term defined as an actual/ideal flux ratio (β). A recent study [14] revealed that β can be determined from flux at zero applied pressure (FO conditions) and permeability coefficient (A) and that J_{wa} and W_a curves as function of applied pressure derived by Eqs. (5) and (6) are consistent with those received by rigorous theoretical model calculations; many of which were reported [15–25] in recent years for advanced PRO–TFC membranes.

$$W = J_w \times p_a \tag{1}$$

where J_w is for water flux (Lmh) across the membrane, $\Delta\pi$ (bar)—osmotic pressure gradient and p_a(bar)—applied hydraulic pressure

$$J_w = A \times (\Delta\pi - p_a) \quad (2)$$

$$J_s = B \times (C_D - C_F) \quad (3)$$

$$S = t_s \times \tau/\varepsilon \quad (4)$$

$$J_{wa} = \beta \times A \times (\Delta\pi - p_a) \quad (5)$$

$$W_a = \beta \times A \times (\Delta\pi - p_a) \times p_a \quad (6)$$

1.3. PRO hydroelectric power generation methods

The conceptual approach of the conventional PRO technology conceived by Loeb [1–3] and practiced today [8–13] is illustrated schematically in Fig. 1 with ERD means of the types displayed in Fig. 2 and the very recently reported [26–28] new approach to PRO in closed circuit is described schematically in Fig. 3(A) with a single side conduit (SC) and in Fig. 3(B) with two alternating SCs. In the conventional method pressurized HSF ("draw") is created by means of the high salinity feed pump (HSF-P), energy recovery device (ERD), and booster pump (BP) with a major role played by ERD whereby power from the HSDF effluent is

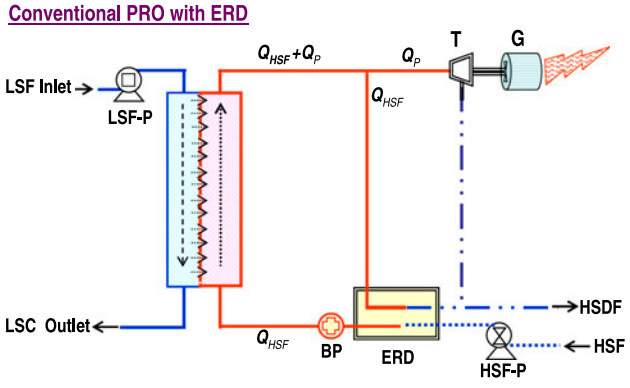

Fig. 1. A schematic design of a single module conventional PRO apparatus with pressurized sections indicated in red and non-pressurized sections in blue. Abbreviations: LSP, low salinity feed ("feed" solution); LSC, low salinity concentrated (concentrated "feed" effluent); HSF, high salinity feed ("draw" solution); HSDF, high salinity diluted feed (diluted "draw" solution); *T*, turbine; *G*, generator; HSF-P, high salinity feed pump; LSP-P, low salinity feed pump; BP, booster pump; ERD, energy recovery device; *Q*, flow stream of cited components with Q_P pertaining to permeation flow across the semipermeable membrane.

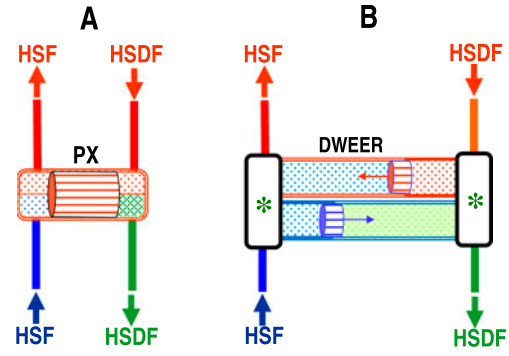

Fig. 2. Schematic design of ERD systems such as PX [A] and DWEER [B] of common use in conventional PRO and SWRO desalination plants—in reference to PRO, red signifies pressurized sections, blue non-pressurized sections associated with HSF and green non-pressurized sections associated with HSDF effluent.

restored in the HSF. The most commonly used ERD means for conventional PRO as well as for SWRO desalination applications are the isobaric energy recovery pressure exchanger PX by ERI [29] and the dual work energy exchange recovery DWEER by Flowserve [30] of the respective schematic designs in Fig. 2(A) and Fig. 2(B). The PX device is a pressure exchanger containing a fast-rotating ceramic disk wherein the pressure of the disposed HSDF effluent is conveyed to the HSF with claimed power conversions efficiency up to 98%. The DWEER device is essentially a positive displacement pump of high hydraulic efficiency up to 98% which is powered by the pressurized stream of the HSDF effluent from the PRO unit. Conventional PRO requires ERD of very high energy recovery efficiency in order to become economically effective. The SCs in the closed circuit PRO (CC-PRO) process (Fig. 3(A–B)) are expanded pipe sections with valve means to enable their engagement with the closed circuit for supply of pressurized HSF ("draw") without need of ERD. The CC-PRO design with a single SC (Fig. 3(A)) enables recycling of HSDF through the PRO module with occasional replacement of pressurized HSDF by pressurized HSF with near absolute energy efficiency and without need of ERD. The CC-PRO design with two alternating SCs (Fig. 3(B)) enables continuous supply of pressurized HSF to the inlet of the module with simultaneous removal of HSDF (diluted "draw") from its outlet with near absolute energy efficiency and without need of ERD. The near absolute energy conversion efficiency of the CC-PRO process is associated with the negligible energy requirements during the compression/decompression of the SCs which takes place under hydrostatic conditions. The purpose of the CP in CC-PRO is to generate cross flow along the module without which the

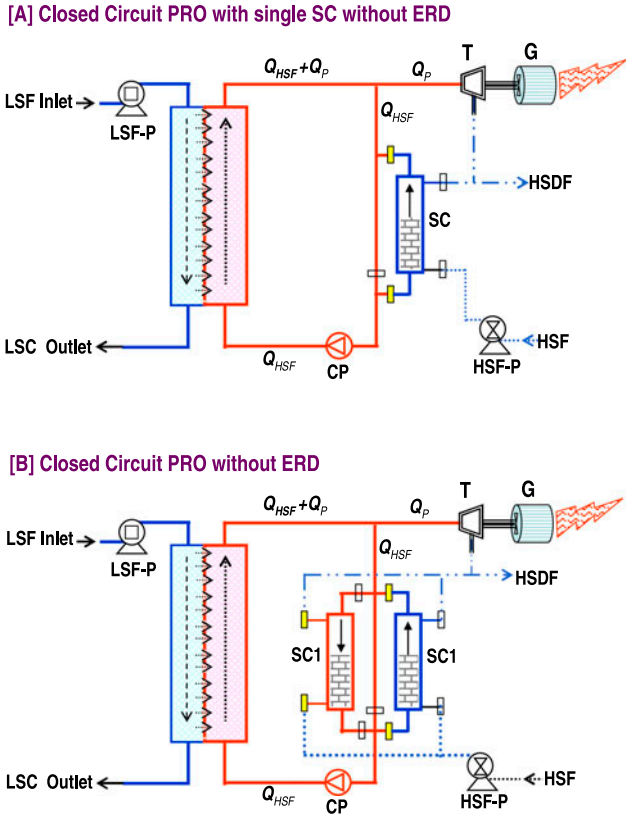

Fig. 3. Schematic designs of single module closed circuit PRO apparatus of one [A] and two [B] side conduit configurations. Abbreviations in additions to those already cited in Fig. 1: CP—circulation pump; SC—side conduit; small rectangles, actuated valve means except for HSF inlets to SCs where one-way check valves are used instead of actuated valves.

PRO process is not possible. Generation of cross flow in CC-PRO by CP requires compensation for flow induced pressure losses along the module (Δp_M), or the module inlet–outlet pressure difference. In general, Δp_M can be kept low by module design features of low flow induced pressure losses. The role of CP in CC-PRO does not include pressure boosting as in the case of BP in the conventional method where the operational pressure of the pump is determined by $\Delta p_M + \Delta p_{ER}$ of which latter is the compensated pressure loss in the ERD as function of its efficiency.

The deceptive similarity between the SC configuration in CC-PRO according to Fig. 3(B) and conventional PRO according to Fig. 1 with ERD made of DWEER according to Fig. 2(B) does create an optical illusion as if the SC in the former functions as a DWEER like ERD system and this is not the case for the following reasons:

(1) No pressurized flow is discharged from the CC-PRO unit according to either Fig. 3(A) and/or Fig. 3(B) and therefore, no need exists for energy recovery.
(2) The SCs in CC-PRO are expanded pipe sections of the closed circuit of same inlet and outlet flow rate (Q_{HSF}) created only by the CP at a small pressure difference (Δp_M) due to flow induced pressure losses along the module, or in simple terms, CP compensates only for the small pressure loss along the module and therefore, its function is different from that of the BP pump in the conventional design (Fig. 1).
(3) The flow created inside the SCs of CC-PRO (Fig. 3(A–B)) by the CP requires an external electric power supply; whereas, the DWEER system (Fig. 2(B)) in conventional PRO (Fig. 1) is a pressurizing pump powered by the continuous stream of the pressurized HSDF effluent—a stream not found in CC-PRO.
(4) The alternating engagement of SCs in CC-PRO (Fig. 3) proceeds with negligible losses of hydrostatic compression/decompression energy, or in simple terms, essentially no lost energy of need for recovery by DWEER exists in said process.

The aforementioned imply that CC-PRO is a batch process of near absolute energy efficiency without need for energy recovery and the making of such a process continuous achieved by means of the alternating engagement of SCs with negligible energy since compression/decompression of the SCs takes place under hydrostatic conditions.

1.4. PRO Module performance

The same PRO module applies for conventional and CC-PRO and the performance of such a module as function of its semipermeable membrane characteristics can be analyzed from the stand point of permeation flux in the pressurized section of such a module, irrespective of whether flux decline is uniform or not, according to undisputed performance features as followed:

(1) *PRO module inlet parameters:* inlet concentration (C_i), osmotic pressure difference ($\Delta\pi_i$), and flow rate (Q_i) are fixed and independent of applied pressure (p_a) which only effects the net driving pressure term NDP_i [$=\Delta\pi_i - p_a$].

Ideal water flux at module inlet under zero applied pressure conditions according to Eq. (2) is defined by the fixed product $A \times \Delta\pi_i$. Actual flux at module inlet according to Eq. (5) is defined by the product $\beta \times A \times \Delta\pi_i$; wherein, β is the actual/ideal flux ratio.

(2) *PRO module outlet parameters:* outlet concentration (C_o), osmotic pressure difference ($\Delta\pi_o$), and flow rate (Q_o) are different from the fixed inlet parameters with $C_o < C_i$, $\Delta\pi_o < \Delta\pi_i$, $Q_o > Q_i$, and $NDP_i > NDP_o$ and the difference between inlet and outlet parameters translates to variations of NDP and water flux during the PRO progression.

(3) *PRO module ideal power:* ideal power availability is the product of $(Q_o–Q_i) \times p_a$ or $Q_p \times p_a$; wherein, Q_p stands for the permeation flow determined by the average flux in the module with ideal power density (W) expressed by the product $A \times (\Delta\pi–p_a) \times p_a$ derived from Eqs. (1) and (2).

(4) *Applied pressure of ideal peak power:* the applied pressure of ideal peak power density in PRO can be determined by differentiating the power expression $w = A \times (\Delta\pi–p_a) \times p_a$ with respect to p_a whereby [4] peak power is attained at $p_a = \Delta\pi/2$ and corresponds to $A \times [\Delta\pi]^2/4$. The calculated ideal maximum applies to an ideal membrane of no detrimental effects in a module with $NDP_{av} = \Delta\pi/2$ possible only when $NDP_i = \Delta\pi$ and $NDP_o \approx 0$, or in simple terms, when the module inlet and outlet concentration difference $[C_i–C_o]$ is very small.

(5) *Applied pressure of actual peak power*: actual PRO peak power should take account of all the detrimental effects on the membrane performance such as expressed by β in Eq. (6) and of the module outlet parameters of concentration (C_o), osmotic pressure ($\Delta\pi_o$), and net driving pressure (NDP_o) under economically feasible single pass PRO conditions of $50 \pm 10\%$ permeate in the HSDF (diluted "draw") expressed by the term α in Eq. (7). Meeting the aforementioned requirements for a viable PRO process implies an actual applied pressure peak power different from the theoretical projection and/or experimental results of low percent α.

(6) *PRO module stationary state conditions:* a PRO module of a specific membrane at a defined applied pressure will create stationary state conditions manifested by fixed flow ratio (δ) of HSF ("draw" or CP) to permeate expressed by Eq. (8) and α expressed by Eq. (7). According to Eqs. (7) and (8), the fixed relationships between δ and α are expressed by Eqs. (9) and (10). In conventional PRO wherein the flow rate of the "draw" solution ($Q_{draw} = Q_{HSF}$) is maintained constant according to the flow capacity of the ERD, alteration of applied pressure is accompanied by permeation flow variations and changes of both δ and α, or in simple terms, each applied pressure selection generates a different stationary state conditions inside the PRO module. In contrast with the conventional PRO method wherein the module inlet flow rate of the "draw" solution (HSF) is confined by the ERD, CC-PRO can be operated with any desired HSF flow rate ($Q_{HSF} = Q_{CP}$) dictated only by the selected flow rate of CP(vfd) under fixed or variable δ ratio of unchanged or changing stationary state conditions, respectively.

$$\alpha\ (\%) = [(Q_{HSDF} - Q_{HSF})/Q_{HSF}] * 100 = Q_p/Q_{HSDF} * 100 = Q_p/(Q_p + Q_{CP}) * 100 = (Q_o - Q_i)/Q_o * 100 \quad (7)$$

$$\delta = Q_{HSF}/Q_p = Q_{CP}/Q_p \quad (8)$$

$$\delta = (100 - \alpha)/\alpha \quad (9)$$

$$\alpha = 100/(\delta + 1) \quad (10)$$

1.5. Scope and prospects for CC-PRO with SW–RW like salinity gradients

The preset study explores the scope of prospects of CC-PRO for the worldwide most common salinity gradient system comprising of seawater and river water which corresponds to an osmotic pressure difference at inlet to PRO module of 25 ± 1 bar. In order to outline present PRO maximum peak power generation prospects of SW–RW, the study described hereinafter focuses on the recently reported [18] TFC–PRO membrane MP # 1 ($A = 5.81$ Lmh/bar, $B = 0.88$ Lmh and $S = 349$ μm) of the highest reported permeability coefficient known today and analyzes ideal, actual, and net electric power output projections under different PRO operational conditions in the context of CC-PRO as compared with conventional PRO. The ultimate objective of the model analysis under review is to assess the net PRO electric power availability by CC-PRO and conventional PRO with the best reported TFC–PRO membrane [18] under practical PRO

conditions of α = 50 ± 10% permeate in HSDF (diluted "draw") with all energy consumption requirements of auxiliary pumps accounted for in the final power output of the system.

2. SW–RW PRO module performance with the TFC-PRO MP # 1 membrane of A = 5.81 Lmh/bar, B = 0.88 Lmh and S = 349 μm

Recently Yip et al. reported [18] a comprehensive study describing the performance of a newly prepared TFC-PRO membrane of A = 5.81 Lmh/bar, B = 0.88 Lmh, and S = 349 μm with a theoretical peak power density of 10 W/m^2 in a salinity gradient system comprising 0.55 M–0.96 mM NaCl concentrations typical of a SW–RW system. The only experimental data provided in the report was that of the actual flux (~55 Lmh) at zero applied pressure. Data extracted from the expanded theoretical curves of flux and power density of said report [18] at the applied pressure points 0.0; 2.5; 5.0; 7.5; 10.0; 12.5; 15.0; 17.5; 20.0; and 25.0 bar revealed the theoretically calculated actual flux and power density (in parenthesis) of 55(0.00); 50(3.47); 45(6.25); 40(8.33); 34 (9.44); 29(10.0); 23(9.58); 18(9.75); 11(6.11); 4.5(2.81), and 0.0(0.0) Lmh(W/m^2), respectively. More recently, it has been shown [14] that a projection almost identical to that of Yip et al. can be generated by Eqs. (5) and (6) using β = 0.374 (actual/ideal flux ratio) derived from the reported [18] experimental flux at zero applied pressure for said membrane. In order to better understand the PRO module performance characteristic of the MP # 1 membrane, a CC-PRO model analysis was performed for the salinity gradient 0.55 M–1.0 mM NaCl in the HSF/permeate flow ratio (δ) range 0.75–60 with percent permeate in HSDF (α) of 57.14–1.64%, respectively. The CC-PRO analysis over a wide δ or α range was necessary in order to establish net electric power output under practical PRO operational conditions of economic feasibility with full count taken of power produced and consumed during the PRO operation. It should be pointed out that the part of the generated PRO power consumed by the auxiliary pumps in the system under review is an essential parameter for assessing the net electric power availability of the PRO technology and this parameter relates to the practical operational conditions and to the flow ratio δ (or α) in particular which dictates the flow rates of the auxiliary pumps. Comparison between net electric power availability of CC-PRO and conventional PRO was established in the context of the ERD efficiency of the latter method.

2.1. SW–RW CC-PRO module performance using the TFC-PRO MP # 1 membrane under fixed flow ratio δ = 1.0 of α = 50% (50% Permeate in HSDF)

The already reported [28] theoretical model data base for CC-PRO simulations is applied in Table 1 in the context of the SW–RW like salinity gradient system comprising of 3.26% (~0.55 M)–0.006% (1.0 mM) NaCl solutions under fixed HSF/permeate flow ratio δ = 1 of 50% permeate in HSDF (α = 50%) in a module having a membrane of A = 5.81 Lmh/bar, B = 0.88 Lmh, S = 349 μm, and β = 0.374. The module described in the Table 1 is equivalent to that of the commercial hollow-fiber TOYOBO HJ-9155-PI open-ended configuration module [31] with an estimated 42 m^2 membrane surface area; wherein, the membrane inside the module is of the cited parameters instead of the cellulose triacetate membrane found in the commercial module. The specific data in the table describes the module performance at an applied operational pressure of 11 bar with ideal and actual average module flux of 48.9 and 18.3 Lmh, respectively, under which conditions the membrane power density is 5.59 W/m^2 and net electric power availability 3.93 W/m^2 after accounting for the efficiency (90%) of the turbine–generator (T–G) and the power consumption of the auxiliary pumps. The entire CC-PRO simulation results of said system with δ = 1.0 and α = 50% over the applied pressure range 0–24 bar are revealed with respect to flux in Fig. 4(A), power density in Fig. 4(B), net electric power in Fig. 4(C), module concentrations in Fig. 5(A), module osmotic pressures in Fig. 5(B), module NDP in Fig. 5(C), HSF and Permeate flow rates in Fig. 5(D), HSF/Permeate flow ratio in Fig. 5(E) and % Permeate in HSDF in Fig. 5(F).

2.2. SW–RW CC-PRO module performance with the TFC-PRO MP # 1 membrane in the δ range 0.75(57.14%)–60 (1.54%) of α in parenthesis

The theoretical model data base for CC-PRO simulation displayed in Table 1 in the context of the SW–RW like salinity gradient system comprising 3.26% (~0.55 M)–0.006% (1.0 mM) NaCl solutions was extended to include complete sets of actual PRO power density projections as function of applied pressure under module stationary state conditions in the δ range 0.75 (57.14%)–60 (1.54%) of α in parenthesis by entering the selected δ value in the appropriate location of flow ratio in the table. The model analysis comparative results of actual PRO power density availability as function of δ and α in the range 0.75 (57.14%)–60 (1.54%) for said SW–RW salinity gradient system are displayed in Fig. 6. The cited residence

Table 1
Theoretical model data base for CC-PRO simulation exemplified with SW–RW like salinity gradient system of 3.26% (~0.55 M)–0.006% (1.0 mM) NaCl solutions under fixed flow ratio HSF/permeate (δ) = 1.0 in a module with a membrane of A = 5.81 Lmh/bar, B = 0.88 Lmh, S = 349 μm, and β = 0.374

3.26	% NaCl HSF	26.1 bar OP
0.006	% NaCl LSF	0.04 bar OP
		26.0 bar Δπ

Design & Membrane Data

1	Number of Modules
1	No of Membrans per Module
205	cm length of module
30	cm, inner diameter of module
145	liter, gross volume of module
50.0	% membrane volume in module*
72.4	liter net volume of Module
42.0	m2, membrane surface per module
42.0	m2 total surface area of design

* Assumed

LSF-LSC Performance Data

Module	Unit	
0.961	0.96	m3/h LSF Inlet Flow
0.006	0.01	% LSF inlet Salinity
0.192	0.19	m3/h LSC outlet Flow
0.028	0.03	% LSC outlet Salinity
0.769	0.77	m3/h Permeation Flow
0.017	0.02	% mean Salinity (inlet+outlet)/2
0.135	0.13	bar mean Δπ=(inlet+outlet)/2
0.20	0.20	Ratio Q_{LSC}/Q_{LSF} $Q_p=Q_{LSF}-Q_{LSC}$
80	80	% permeate from LSF

PRO Membranes Detrimental Effect

0.374	Ratio Actual/Ideal assumed
62.6	% Detrimental Effects

Fixed Flux per Single Module

18.3	lmh Flux (Selected average)
0.77	m3/h (Q_p) Module average Permeate
12.81	lpm Module average Permeate

Recycling Flow of Single Module

0.77	m3/h recycling flow (Q_{CP})
12.8	lpm recycling flow of module (Q_{CP})
5.7	minute complete volume recycle
1.00	Selected Flow Ratio (Q_{CP}/Q_p)
5.653	min., HSF residence in module

Flow of Entire Design

0.77	m3/h Permeate Flow of entire unit
0.77	m3/h Recycling Flow of entire unit
50.00	% permeate in HSDF

HSF - HSDF Module Inlet & Outlet Data

3.26	% HSF Module Inlet
26.04	bar Δπ Module Inlet
1.63	% HSDF Module Outlet
12.8	bar Δπ Module Outlet
2.45	% HSDF average
19.4	bar Δπ Module average

8.00	Δπ(bar)/C(%) - SW Conversion factor
8.00	Δπ(bar)/C(%) - BW Conversion factor

Power Demand of CC-PRO PUMPS

Performance	HSP	LSP	CP
m3/h	0.77	0.96	0.77
bar	0.50	0.50	0.50
Efficiency assumed	0.75	0.75	0.75
Watt	14.23	17.79	14.23

TOTAL-Pumps Power Demand (W)	46.3
TOTAL-Pumps Power Density (W/m2)	1.10
Actual PRO only (W/m2)	5.59
Pumps Demand (W/m2)	-1.10
Turbine-Generator-10% PRO loss	-0.559
Net Electric Power (w/m2)	3.93
Energy per m3 Permeation (kWh/m3)	0.215
Energy per m3 LSF (kWh/m3)	0.172

PRESSURE, NDP and FLUX DATA

Permeability Coefficient (l/m2/h/bar)				5.81
Module Parameters		Ideal		Actual
Type		NDP	FLUX	FLUX
Applied -bar	11.0	bar	lmh	lmh
Δπ MOD Inlet	26.0	15.0	87.4	32.7
Δπ MOD Outlet	12.8	1.8	10.5	3.9
Δπ MOD average	19.4	8.4	48.9	18.3
CC-PRO Selected average Flux				18.3

time (T) in the figure is derived from the intrinsic free volume of the module (72.4 L) and flow rate of HSF (L/min) and expresses the residence time from inlet to outlet of specific HSF solute constituents inside the PRO module. Actual PRO power density variations are displayed in Fig. 7 as function of the HSF/permeate (δ) flow ratio [A], flow rates of permeate and HSF [B], percent permeate (α) in HSDF [C], and residence time (T) of HSF constituents inside the module [D]. Noteworthy features revealed in Figs. 6 and 7 are the declined actual PRO power availability with decreased flow ratio (δ), increased percent permeate in HSDF (α) and declined residence time (T) of HSF constituents inside the module. Decline of PRO power density availability as function of δ, α, and T also includes maximum peak power availability and its shifting towards lower applied pressures. Another noteworthy feature of considerable practical significance is the need for much greater flow rate of HSF compared with that of permeate ($Q_{HSF} >> Q_P$) to achieve very high peak power; however, this is achieved at the expense of much greater energy consumption by CP and the HSF-P auxiliary pump.

2.3. Net electric power availability of the CC-PRO module with the TFC-PRO MP # 1 membrane in the δ range 0.75 (57.14%)–60 (1.54%) of α in parenthesis

The theoretical model data base of CC-PRO simulation for the SW–RW like salinity gradient system displayed in Table 1 also contains information concerning the power consumption requirements of the auxiliary pumps (HSF-P, LSF-P, and CP) displayed in the schematic designs of such units in Fig. 3(A–B). Accordingly, the net electric power availability of CC-PRO takes account of PRO power availability, the efficiency of the T–G, and the power requirements of the cited auxiliary pumps. The theoretical model data base in Table 1 does allow a direct assessment of the net electric power availability of the CC-PRO unit by the computed balance of power produced and consumed and the results for the SW–RW salinity gradient under consideration are revealed in Fig. 8 for a module with MP # 1 membrane under operational conditions in the δ range 0.75 (57.14%)–60 (1.54%) with α cited in parenthesis. The data in Fig. 8 reveals the significant role played by the auxiliary systems of the CC-PRO unit in

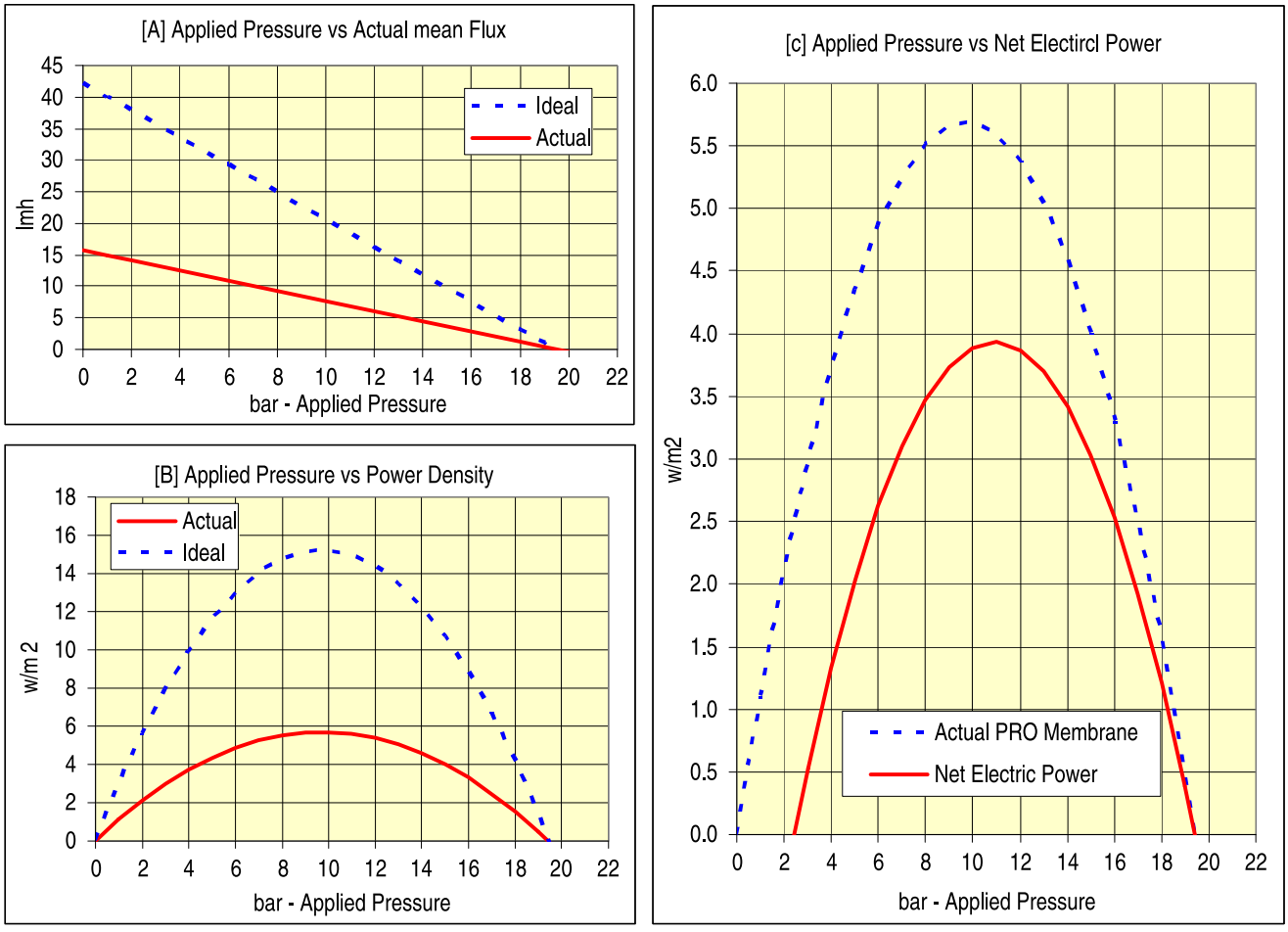

Fig. 4. Applied pressure vs. flux (A), power density (B), and net electric power (C) according to the data base in Table 1 under the conditions of $\delta = 1.0$; $\alpha = 50\%$.

determining the net electric power availability of such a hydroelectric power generation system with increased flow ratio (δ) of lower percent permeate in HSDF (α) resulting in a sharp decline of net electric power availability due to the increased power requirements of the auxiliary pumps. The negative power section displayed in Fig. 8 illustrates the diverted PRO power to compensate for the power requirements of the auxiliary pumps. The operational parameters of the auxiliary pumps assume efficiency of 75% and pressure of 0.5 bar with T–G efficiency of 90% according to flow rates defined by the PRO process conditions. The net electric power availability of the CC-PRO system under review is confined to the flow ratio (δ) range 0.75 (57.44%)–2.5 (28.57%) of cited (parenthesis) percent permeate in HSDF (α).

2.4. Net electric power availability of CC-PRO vs. conventional PRO as function of ERD efficiency using a module with MP # 1 membrane for the salinity gradient 3.26% (~0.55 M) – 0.006% (1.0 mM) NaCl at $\delta = 1.0$ of $\alpha = 50\%$

Hydroelectric power in PRO irrespective of method is expressed by Eq. (11) and in case of conventional PRO some of this power is required by the BP in order to compensate for the ERD losses expressed by Eq. (12), where f stands for the efficiency ratio of the turbine–generator (f_{TG}) and ERD (f_{ERD}). Accordingly, the ratio of lost hydroelectric power due to the efficiency of the ERD is expressed by η in Eq. (13). The electric power output of conventional PRO ($W_{TG\text{-}CONV}$) can be deduced from that of CC-PRO by Eq. (14) which takes

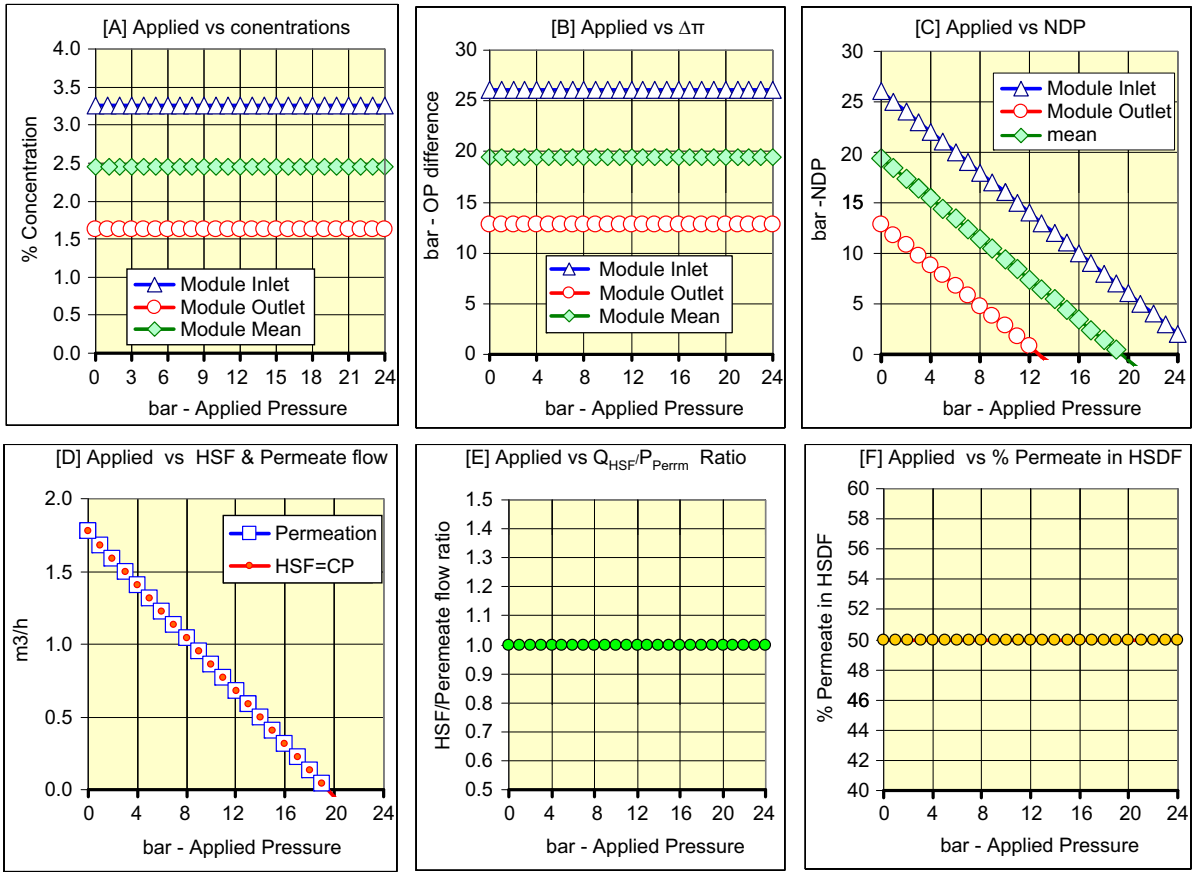

Fig. 5. Applied pressure vs. module concentrations [A], module osmotic pressures [B], module NDP [C], HSF, and permeate flow rates [D], HSF/Permeate flow ratio [E] and % Permeate in HSDF [F], according to the data base in Table 1 under the conditions of $\delta = 1.0$; $\alpha = 50\%$.

into account the fraction of PRO electric power lost as function of ERD efficiency. In light of the aforementioned, the net electric power availability of conventional PRO can be expressed by Eq. (14), less the power demand of the auxiliary pumps HSP-P, LSF-P, and BP in its flow circulation function as distinguished from its pressure boosting function of lost ERD pressure. The comparative results of the net electric power availability of CC-PRO of no EDR and conventional PRO as function of its EDR efficiency for the MP # 1 membrane in the salinity gradient system 3.26% (~0.55 M)–0.006% (1.0 mM) NaCl at $\delta = 1.0$ of $\alpha = 50\%$ are furnished in Fig. 9.

$$W_{TG} = Q_P \times p_a \times f_{TG} \tag{11}$$

$$W_{ERD-LOSS} = Q_{HSF} \times p_a \times (1 - f_{ERD}) = Q_P \times \delta \times p_a \times (1 - f_{ERD}) \tag{12}$$

$$\eta = \delta \times [1 - f_{ERD}]/f_{TG} = [100 - \alpha/\alpha] \times [(1 - f_{ERD})]/f_{TG} \tag{13}$$

$$W_{TG-CONV} = (1 - \eta) \times Q_P \times p_a \times f_{TG} \tag{14}$$

The information revealed in Fig. 9 demonstrates that the same maximum peak of net electric power availability of 3.93 W/m^2 at 11 bar applied pressure for CC-PRO and convention PRO is attainable only when the latter operates with ERD efficiency of 100%. Declined ERD efficiency causes a sharp drop of the net electric availability of conventional PRO as clearly evident from the curves in Fig. 9. The effectiveness of ERD in conventional PRO could not be assessed in absence reported experimental information which should have been available for the demonstration PRO plants in Norway [8–10] and Japan [11–13]. In contrast

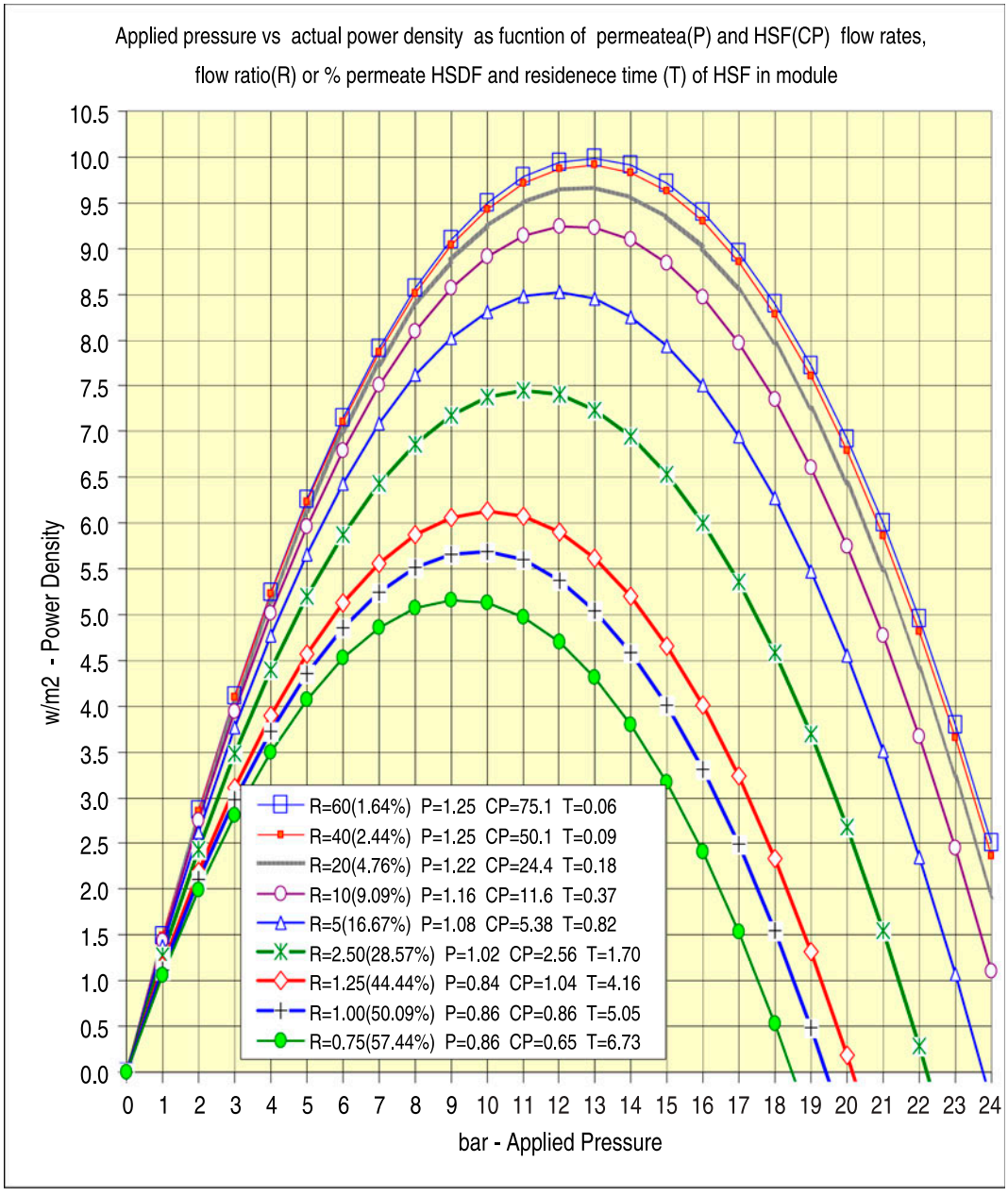

Fig. 6. Applied pressure vs. actual PRO power density according to the data base in Table 1 under stationary state conditions of different δ (0.75R→60R) and α (57.4%←1.64%). Abbreviations: R, stands for flow ratio (δ); P, for permeation flow in m^3/h; CP, for HSF ("draw") flow rate in m^3/h; and T, for residence time (min) of the HSF constituents inside the module at peak power.

with conventional PRO, the near absolute energy efficiency of the CC-PRO process is achieved without need of ERD in the absence of pressurized flow emission from which energy needs to be recovered.

3. Discussion

The application of widespread worldwide salinity gradients as fuels for large-scale clean renewable power generation by means of membrane-based PRO

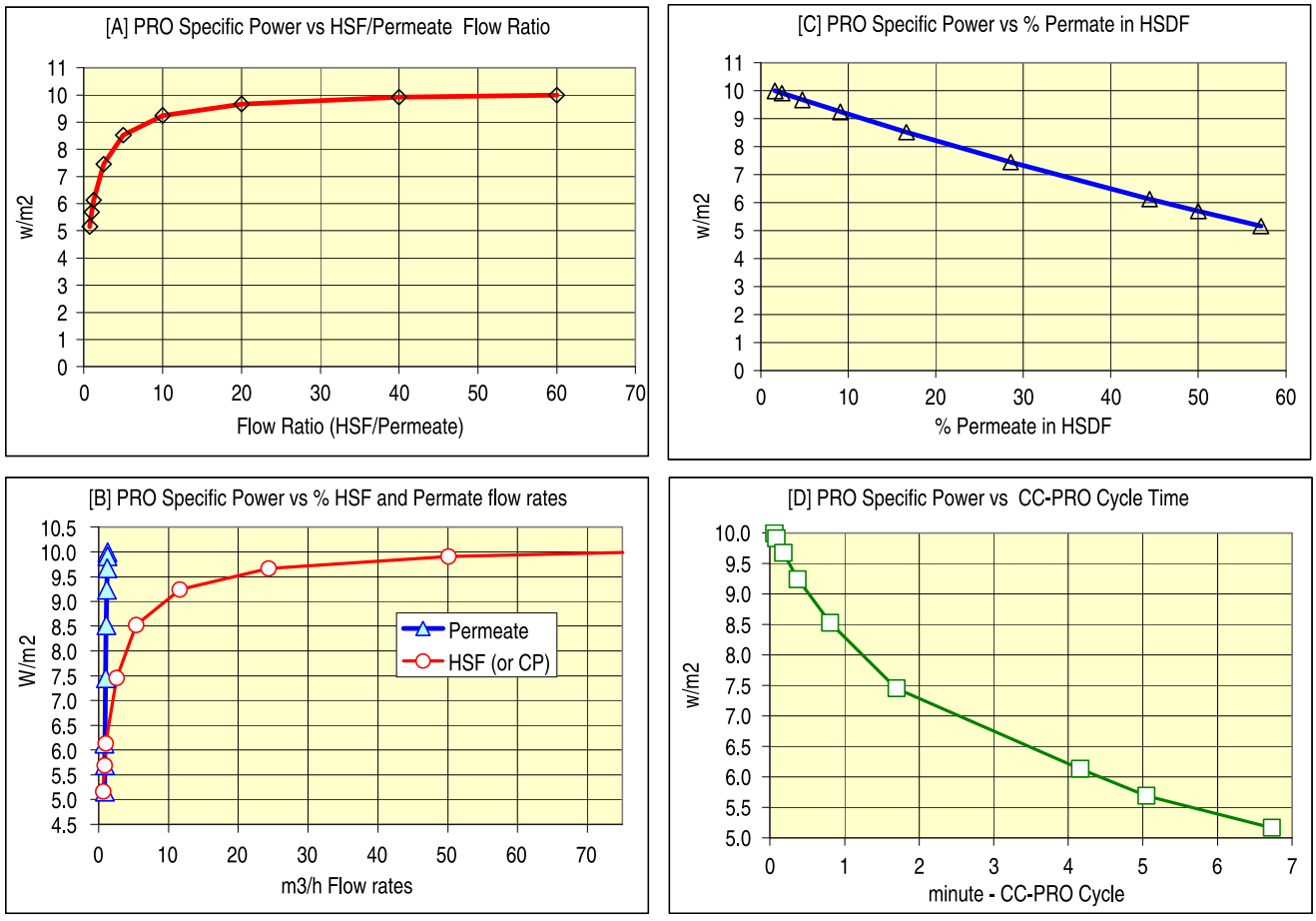

Fig. 7. Actual PRO peak power density as function of HSF/permeate (δ) flow [A], flow rates of permeate and HSF [B], percent permeate (α) in HSDF [C], and residence time (T) of HSF solute particles inside the module at peak power [D].

technologies is a novel concept of enormous economic prospects and considerable environmental consequences and the present study focuses primarily on the assessment of SW–RW salinity gradients for such a noteworthy purpose. Knowledge of the current status of SW–RW PRO requires the identification of the best available membrane for such an application and the evaluation of its performance characteristic which define the maximum present prospects. Since new advanced PRO membranes are reported at an ever growing frequency, the status of this area is bound to change rather rapidly with more advanced membranes of better performance leading to greater future prospects. Recently, Yip et. al. reported [18] an advanced TFC–PRO membrane labeled MP # 1 of $A = 5.81$ Lmh/bar, $B = 0.88$ Lmh, and $S = 349$ μm with theoretical model peak power projection of 10 W/m^2 at an applied pressure of 13 bar for SW–RW like salinity gradient which is presently the best known membrane for said application. MP # 1 was selected as reference in the current study since it defines the present status of maximum PRO power generation mile stone on route for the making this noteworthy technology commercially available in the near future.

Ideal PRO power density according to existing theory is defined by Eq. (1) in terms of ideal water flux as defined by Eq. (2) solely on the basis of the membrane permeability coefficient (A) and the selected applied pressure. In practice, actual water flux of PRO membrane is found to be much lower than predicted by theory and extensive theoretical model studies of different membranes [15–25] revealed that declined PRO flux arises from detrimental effects of internal (ICP) and external (ECP) concentration polarization origin and the structural features of membranes. Accordingly, actual PRO flux and power is best described by the respective expressions Eqs. (5) and (6); wherein, β stand for an actual/ideal flux ratio parameter which takes account of all the detrimental effects responsible for the declined flux through the

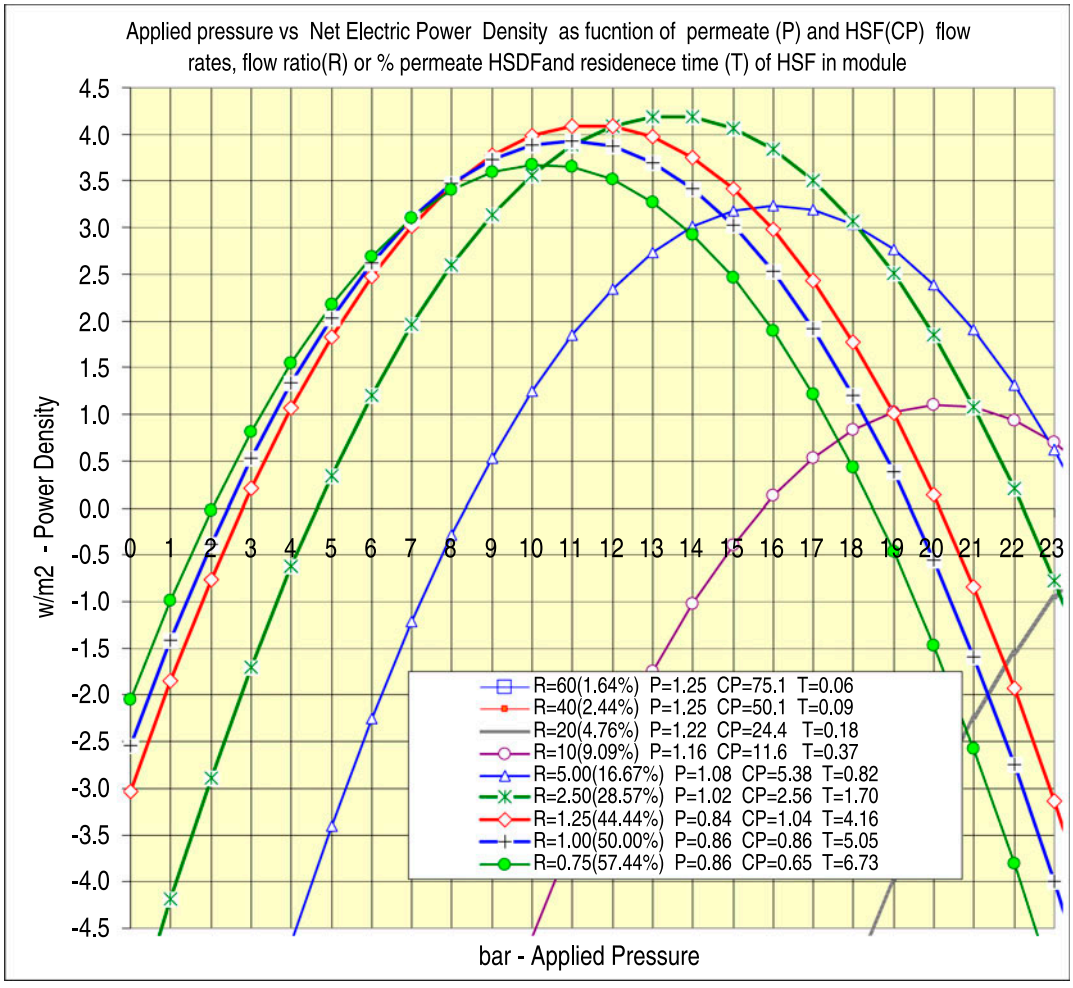

Fig. 8. Applied pressure vs. net electric power availability of the CC-PRO unit according to the database in Table 1 under stationary state conditions of different δ ($0.75R \rightarrow 60R$) and α (57.4←1.64%). Abbreviations: R, stands for flow ratio (δ); P, for permeation flow in m^3/h; CP, for HSF ("draw") flow rate in m^3/h; and T, for residence time (min) of HSF solute particles inside the module at peak power.

membrane. The β terms is easily attainable from A and experimental PRO flux at zero applied pressure under FO conditions and its application for PRO performance projections in the context of Eqs. (5) and (6) for several advanced membranes in different salinity gradients revealed [14] comparative results of high consistency with rigorous theoretical model calculations and experimental data when made available and therefore, confirming the validity of the β–A method for performance evaluation of PRO membranes. The application of the β–A method for the performance evaluation of the same PRO membrane in different salinity gradients revealed declined β with increased osmotic pressure difference ($\Delta\pi$) of the source solutions implying greater detrimental effects on flux as function of increased $\Delta\pi$ and vice versa.

The reported [18] experimental flux at zero applied pressure for MP # 1 of ~55 Lmh in SW–RW ($\Delta\pi \approx$ 26 bar) combined with $A = 5.81$ Lmh/bar provided the basis for the calculated parameter $\beta = 0.374$ according to Eq. (5) and this actual/ideal flux ratio parameter is used hereinafter for the performance evaluation of MP # 1 in the context of the current study. The theoretical model data base for CC-PRO simulations of MP # 1 in SW–RW provided in Table 1 specifically relates to actual/ideal flux ratio $\beta = 0.374$ and $A = 5.81$ Lmh/bar as the footprints of the cited membrane in the salinity gradient system under review. The simulation data base in Table 1 takes into account of all pertinent aspects of the PRO process including a defined module of know free intrinsic volume (72.4 L), a defined membrane ($A = 5.81$ Lmh/bar and $\beta = 0.374$) of

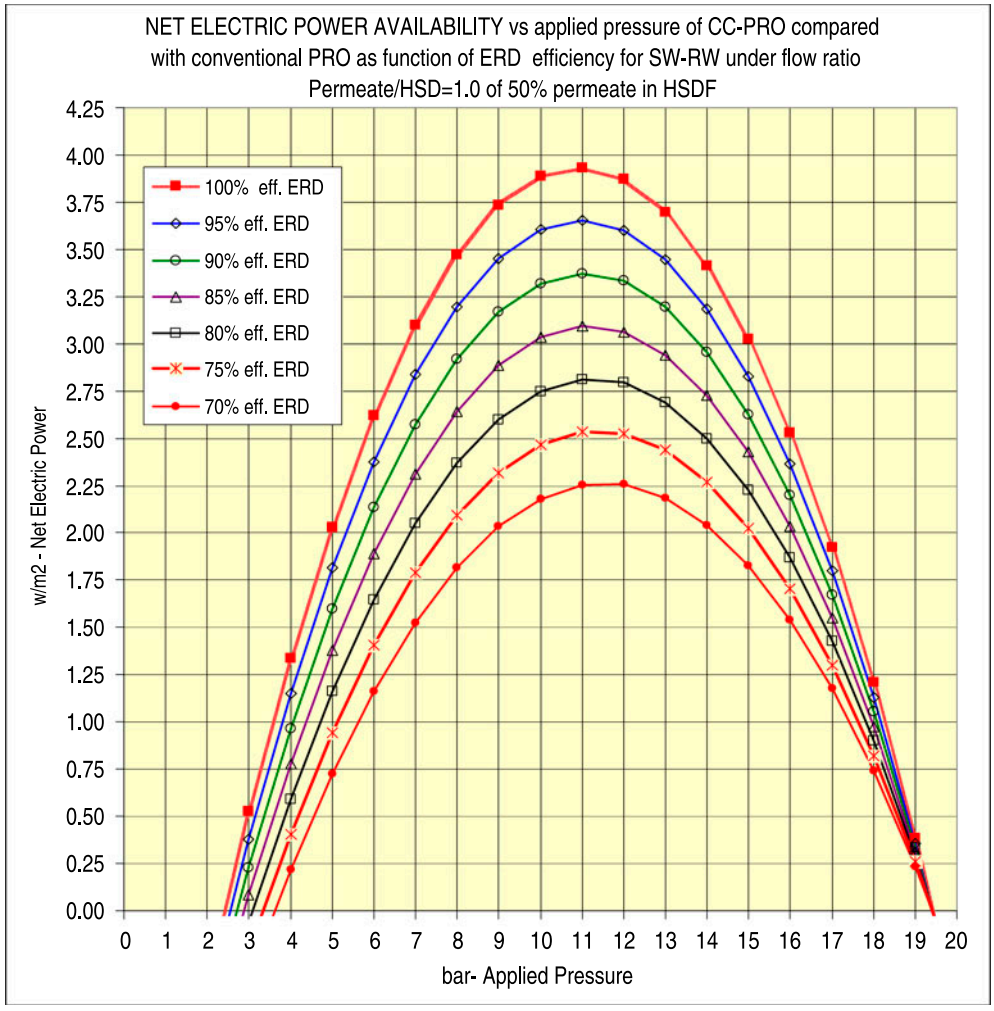

Fig. 9. Net electric power availability vs. applied pressure for CC-PRO compared with conventional PRO as function of ERD efficiency for the SW–RW salinity gradient 3.26% (~0.55 M)–0.006% (1.0 mM) NaCl solutions under HSF/permeate (draw/permeate) flow ratio conditions $\delta = 1.0$ of 50% (α) permeate in HSDF (diluted "draw").

known-surface area (42 m^2), a defined salinity gradient system of known concentrations (3.26–0.006% NaCl) and defined operation conditions under fixed HSF/permeate flow ratio ($\delta = 1.00$). The flow rates data illustrated in Table 1 are for fixed HSF/permeate flow ratio ($\delta = Q_{HSP}/Q_P = 1.00$) PRO operation of unchanged stationary state conditions, irrespective of applied pressure; wherein, $Q_{HSF} = \delta^* Q_P$ and Q_P determined by the actual flux at the selected applied pressure. The flow rates illustrated in Table 1 are said for an average permeation flux of 18.3 Lmh created at a selected applied pressure of 11 bar and manifests the specific flow rates $Q_{HSF} = Q_{CP} = Q_{draw} = 0.77\ m^3/h$, $Q_P = 0.77\ m^3/h$, and $Q_{HSDF} = 1.54\ m^3/h$. The flow rate of LSF at module inlet ($Q_{LSF} = 0.96\ m^3/h$) and LSC at module outlet ($Q_{LSC} = 0.19\ m^3/h$) are also determined by the permeation flux and flow since $Q_P = Q_{LSF} - Q_{LSC}$. The stationary state conditions inside the module at said fixed flow ratio ($\delta = 1.00$) of PRO operation imply unchanged concentrations and osmotic pressures at inlet and outlet of module irrespective of applied pressures with module inlet and outlet net driving pressures (NDP) remain unchanged as long as long as the flow ratio is maintained constant. In simple terms, all aspects related to the membrane, module, and salinity gradient solutions are taken under consideration during the theoretical model simulation of the CC-PRO process without any exception. During the simulation, ideal flux is converted to actual flux by means of β (0.374) and the average flux at each defined applied pressure used to generate the respective permeation flow and the power output according to Eq. (11).

Moreover, the data base also contains pertinent information concerning the auxiliary pumps and their presumed operational pressure and efficiency which combined with the relevant flow rates provide the basis for their power requirements assessment and the net electric power availability projection of the PRO process with an assumed turbine–generator efficiency of 90%.

Ideal and actual flux and power density variations as function of applied pressure during the CC-PRO process with MP # 1 specified in Table 1 for flow ratio $\delta = 1.0$ and $\alpha = 50\%$ (50% permeate in the HSDF) are displayed in Fig. 4(A) and (B), respectively, and the actual membrane power density compared with net electric power availability in Fig. 4(C). Module performance characteristics as function of applied pressure under the specified fixed flow ratio conditions in Table 1 are revealed with fixed inlet, outlet, and average concentrations (Fig. 5(A)) and osmotic pressures (Fig. 5(B)), declined NDP (Fig. 5(C)), and declined flow rates (Fig. 5(D)) of unchanged flow ratio (Fig. 5(E)) and percent permeate in HSDF (Fig. 5(F)). The CC-PRO performance illustration in Table 1 with fixed flow ratio $\delta = 1.0$ of $\alpha = 50\%$ in the practical PRO operational range reveals for MP # 1 and SW–RW peak power of 5.69 W/m^2 at 10 bar applied pressure with 3.89 W/m^2 net electric power availability.

Peak power in CC-PRO is a function of flow ratio selection with increased flow ratio effecting inside the module stationary states of higher outlet concentrations and osmotic pressures of higher average NDP with greater power output. The flow ratio effect in CC-PRO on power generation is illustrated in Fig. 6 with power density curves at δ of 0.75(57.44%); 1.00 (50.00%); 1.25(44.44%); 2.50(28.57%); 5.0(16.67%); 10.0 (9.09%); 20.0(4.76%); 40.0(2.44%); and 60.0(1.64%) with α revealed in parenthesis. The information provided in Fig. 7(A–D) reveals the CC-PRO peak power relationships to flow ratio [*A*], flow rates [*B*], percent permeate in HSDF [*C*] and residence time of HSF constituents [*D*]. Each flow ratio point corresponds to different stationary state conditions inside the PRO module and the maximum peak power of 10 W/m^2 for MP # 1 reported [18] by Yip et al. is attainable only with $\delta > 40$ (Fig. 7(A)) of $\alpha < 2.44\%$ (Fig. 7C) under conditions of little if any practical significance from the stand point of economic feasibility due to the exponentially increased flow rate of HSF ("draw") with δ and the power requirements associated with such increased flow rates. The residence time of HSF constituents at peak power revealed in Fig. 7(D) in the context of CC-PRO is inversely proportional to flow rate of HSF (or CP) with increased flow rates concomitance with decreased residence time and vice versa. Fast flow rates of low residence time associated with high flow ratio (δ) imply module outlet concentrations and osmotic pressures not far below the respective values at module inlet; whereas, CC-PRO operation in the practical range (e.g. $\delta = 1.0$ and $\alpha = 50\%$) is carried out at a relatively low flow ratio with high percent permeate in HSDF under which conditions a reasonable residence time (e.g. ~5 min) of HSF constituents inside the module is made possible and allows for a more economically feasible PRO power generation process.

Noteworthy features in Fig. 6 are the declined applied pressure (13–9 bar) with declined peak power (10.00–5.16 W/m^2), declined flow ratio (δ: 60–0.75), and declined average flux (29.8–20.5 Lmh). The aforementioned trend is consisted with $\Delta\pi$ in Eq. (6) expressing the actual average osmotic pressure difference along the module ($\Delta\pi_{av}$) instead of the difference at module inlet ($\Delta\pi_i$) with a greater $\Delta\pi_i - \Delta\pi_{av}$ difference inducing a shift of applied pressure at peak power towards a lower value. In simple terms, the applied pressure at peak according to the theoretical model simulation data base of CC-PRO in Table 1 is half of the average osmotic pressure difference along the module ($\Delta\pi_{av}/2$) and the relationship of peak power applied pressure to flow ratio is revealed in Fig. 10.

Net electric power output is the single most important parameter of the PRO technology, irrespective of method, and this parameter is the difference between PRO power production and power consumption by the auxiliary systems comprising pumps and a turbine–generator system. The CC-PRO simulated net electric power availability of the MP # 1 SW–RW system as function of applied pressure is disclosed in Fig. 8 in relationships to flow ratio (R), percent permeate in HSDF, flow rates of permeate (P) and HSF (CP) and residence time (*T*) of HSF inside the module at peak power. The highest net electric power availability in the system under review is found in flow ratio (δ) range 0.75 ($\alpha = 57.44\%$)–2.5 ($\alpha = 28.50\%$) where flow rates of HSF ("draw") are relatively low and so are the power consumption requirements of the auxiliary systems. The negative power section displayed in Fig. 8 illustrates the diverted PRO power to compensate for the power requirements of the auxiliary systems. In the model under view in Table 1 the auxiliary pumps are assumed to operate with efficiency of 75% at pressure of 0.5 bar and the T–G system is assumed to operate with 90% efficiency. Net electric power availability of economic feasibility for the CC-PRO system under review is found in the flow ratio (δ) range 0.75 (57.44%)–2.50 (28.57%) of cited (in parenthesis) percent permeate in HSDF (α). The negative power density scale in Fig. 8 manifests a region where

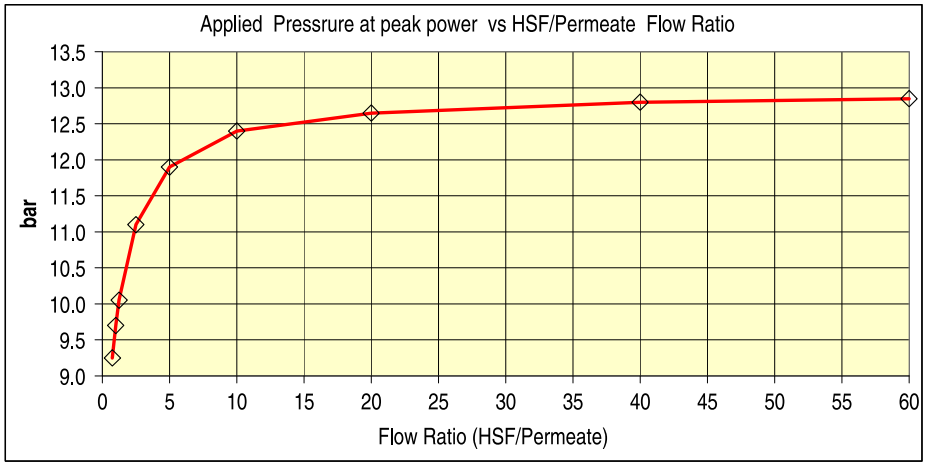

Fig. 10. Peak power applied pressure vs. flow ratio for the MP # 1 SW–RW system according to the theoretical model simulation database of CC-PRO in Table 1.

the power consumption requirements of the auxiliary pumps exceed the PRO power generation and therefore, net electric power availability is negative. The peak power generation levels in the viable PRO flow ratio range are not far apart from each other with operation at $\delta = 1.00–1.25$ ($\alpha = 44.4–50.0\%$) somewhat preferred due to the more effective utility of the HSF component of the salinity gradient.

The effectiveness of PRO is not only a function of membrane and module but also of the performance enabled by the selected method and in this context the comparison between conventional PRO and CC-PRO is noteworthy in particular. Comparison between the cited methods in reference to net electric power availability is furnished in Fig. 9 as function of ERD efficiency of the conventional method. According to the data in Fig. 9, the net electric power availability of conventional PRO equipped with ERD of 100% efficiency is equivalent to that of CC-PRO without ERD, however, the net electric power availability of the former method rapidly declines with decreased ERD efficiency and the effectiveness of such energy recovery means is an issue of utmost importance in the context of conventional PRO. Published information on the conventional PRO hydroelectric power generation demonstration units in Norway (SW–RW) [8–10] and in Japan (SWB–RW like) [11–13] with PX ERD means fail to disclose any information related to the efficiency of energy recovery, although such information is most obviously available. ERD means are extensively used in conventional SWRO desalination plants for the exact same purpose as in case of conventional PRO and therefore, may suggest their effectiveness also in the context of PRO. This subject matter was discussed at considerable length in a recent study [32] wherein extensive comparison is made between the RO energy requirements of conventional SWRO with ERD means and the newly reported [33–35] SWRO–CCD technology of near absolute energy efficiency without such means and this study revealed an overall energy conversion efficiency range of 70–80% in conventional SWRO plants with advanced ERD mean such as PX and DWEER. A comprehensive reported study [36] on the performance of the large SWRO desalination plant in Palmachim (Israel) with its ERT-PX HDYBRID ERD system makes a clear reference to energy conversion efficiency "*just over 76% at the best efficiency point*" and less below the referred point. The aforementioned in the context of the MP # 1 SW–RW PRO system under operational flow ratio conditions of $\delta = 1.0$ ($\alpha = 50\%$) suggests net electric power availability of 3.95 W/m^2 by CC-PRO compared with 2.5 W/m^2 or less by the conventional method and this difference of 36.7% or more electric power availability in favor of CC-PRO is of enormous significance for the making of PRO economically feasible for widespread clean power generation applications.

4. Present status of SW–RW PRO for hydroelectric power generation

Sea and river water combinations are the most immediately available salinity gradient sources for clean energy generation by PRO, an area pioneered [8–10] by Statkarsft in Norway. The present study ascertains the various aspects of SW–RW PRO power generation prospects with respect to the membrane, module and method and the data provided hereinabove for the MP # 1 membrane of the highest thus far

reported [18] peak power density (10 W/m^2) outlines the present status of maximum PRO power generation prospects by PRO.

The peak power for MP # 1 of 10 W/m^2 is suggested by a rigorous theoretical model analysis [18] as well as by a recently reported [14] non-rigorous procedure on the basis of the permeability coefficient (A = 5.81 Lmh/bar) and the actual/ideal flux ratio ($\beta = 0.374$) at zero hydraulic pressure difference across the cited membrane. The current study reveals unambiguously that peak power of 10 W/m^2 for MP # 1 is attainable only under high HSF/permeate ("draw"/permeate) flow ratio (δ) conditions of low percent permeate (α) in the HSDF (diluted "draw") which are of little, if any, practical significance. According to the present study the effective flow ratio (δ) for practical significant SW–RW PRO applications is found in the range of 0.75 (57.4%)–1.25 (44.4%) with percent permeate in HDSF (α) indicated in parenthesis. CC-PRO SW–RW peak power variations as function of flow ratio for MP # 1 according to the present study are exemplified with the declined order of 10.00 W/m^2 at 13 bar ($\delta > 40$; $\alpha < 2{,}44\%$); 8.52 W/m^2 at 12 bar ($\delta = 5.0$; $\alpha = 16.7\%$); 7.45 W/m^2 at 11 bar ($\delta = 2.5$; $\alpha = 28.6\%$); 6.13 W/m^2 at 10 bar ($\delta = 1.25$; $\alpha = 44.46\%$); 5.69 W/m^2 at 10 bar ($\delta = 1.00$; $\alpha = 50.0$); and 5.16 W/m^2 at 9 bar ($\delta = 0.75$; $\alpha = 57.1\%$).

CC-PRO SW–RW net electric power availability (PRO power production less power consumption of auxiliary systems) as function of flow ratio (δ) for MP # 1 according to the present study is confined to a rather limited flow ratio range (δ) exemplified by 4.2 W/m^2 at 13 bar ($\delta = 2.5$; $\alpha = 28.6\%$); 4.1 W/m^2 at 12 bar ($\delta = 1.25$; $\alpha = 44.46\%$); 3.9 W/m^2 at 11 bar ($\delta = 1.00$; $\alpha = 50.0\%$); and 3.6 W/m^2 at 10 bar ($\delta = 0.75$; $\alpha = 57.1\%$).

In contrast with CC-PRO of near absolute energy efficiency, the net electric power availability of conventional PRO is a function of the ERD efficiency as is exemplified for MP # 1 in SW–RW under flow ratio $\delta = 1.00$ ($\alpha = 50.0\%$) by 3.9 W/m^2 at 100%; 3.8 W/m^2 at 95%; 3.4 W/m^2 at 90%; 3.1 W/m^2 at 85%; 2.8 W/m^2 at 80%; 2.4 W/m^2 at 75%; and 2.3 W/m^2 at 70%. Conventional PRO of 100% ERD efficiency is equivalent to CC-PRO with respect to net electric power generation with declined ERD efficiency increasing the effectiveness of CC-PRO over conventional PRO. If ERD efficiency of ~75% characterized in some large SWRO desalination plants applies to conventional PRO as well, the power output of conventional PRO (2.5 W/m^2) vs. that of CC-PRO (3.9 W/m^2) amounts to 59% greater power availability by the latter method and this demonstrates the importance of method selection to maximize the effectiveness of power generation.

Presently, MP # 1 is the membrane of the highest reported SW–RW power density and therefore, its performance characteristics define the ultimate existing boundaries of PRO net electric power availability of 4.0 ± 0.1 W/m^2 made possible by the CC-PRO method in the HSF/permeate flow ratio range 1.00 ± 0.25 of 50 ± 7% permeate in HSDF and most probably 40–55% less by the conventional PRO method.

5. Prospects of SW–RW PRO for hydroelectric power generation

PRO power output according to Eq. (6) depends to a large degree on the effective permeability coefficient expressed by the $\beta \times A$ product; wherein, β is an experimentally derived parameter from the actual/ideal flux ratio of the membrane under FO conditions. The $\beta \times A$ product for MP # 1 of 2.18 Lmh/bar (5.81 × 0.374) comprises an exceptionally high A with

Table 2
CC-PRO power output and net electric power availability projections for membranes of $A = 5.81$ Lmh/bar and actual/ideal flux ratio (β) of 0.374 (MP # 1), 0.500 and 0.75 at different HSF/permeate flow ratio (δ) of different percent permeate in HSDF (α) in the practical range of PRO operations

Module conditions		Pro power				Net electric power		
δ	α (%)	$\beta = 0.374$ (W/m^2)	$\beta = 0.00$ (W/m^2)	$\beta = 0.7502$ (W/m^2)	AP bar (bar)	$\beta = 0.374$ (W/m^2)	$\beta = 0.500$w/m^2 (W/m^2)	$\beta = 0.750$ (W/m^2)
40.0	2.4	9.91	13.25	19.87	13	(−)	(−)	(−)
1.50	40.0	6.48	8.66	12.99	10	3.99	5.34	8.00
1.25	44.4	6.13	8.19	12.29	10	3.98	5.32	7.99
1.00	50.0	5.69	7.61	11.41	10	3.89	5.20	7.79
0.75	57.1	5.16	6.89	10.34	9	3.59	4.80	7.20

Comments: AP, stands for applied pressure; (−) symbolizes negative values; and the column labeled $\beta = 0.374$ is that of MP # 1.

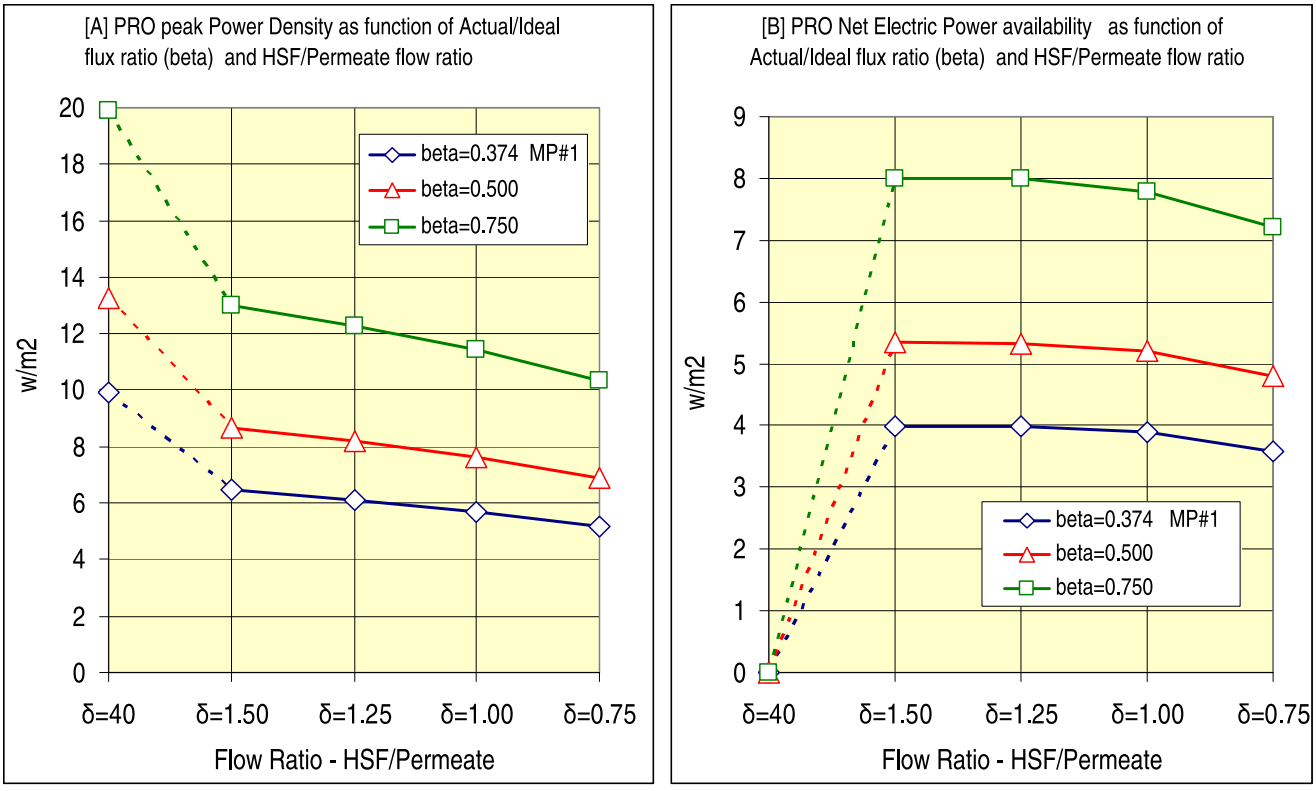

Fig. 11. CC-PRO peak power [A] and net electric power availability [B] as function of HSF/permeate flow ratio for PRO membranes with $A = 5.81$ Lmh/bar of actual/ideal flux ratio (β) of 0.374, 0.500, and 0.750.

a modestly low β and the retention of A with improvements of β should open the door to more effective membrane for PRO applications. The scope for PRO application is suggested in Table 2 for membranes of the same A(5.81 Lmh/bar) as for MP#1 but with actual/ideal flux ratio (β) of 0.500 and 0.750 compared with 0.374 for MP#1 and the results are compared in Fig. 11 in terms of peak power vs. flow ratio as function of actual/ideal flux ratio (β).

Improved SW–RW PRO performance compared with that of MP#1 is expected for membranes of $\beta \times A > 2.18$ Lmh/bar, or greater than that revealed for MP#1. The projections made in Table 2 and Fig. 11(A,B) are for membranes with the same A (5.81 Lmh/bar) of increased β (0.374–0.500–0.750) and $\beta \times A$ (2.18–2.91–4.36) for increased PRO power (5.69–7.61–11.41 W/m^2) and net electric power availability (3.89–5.20–7.79 W/m^2) under conditions of $\delta = 1.00$ and $\alpha = 50\%$ of economic viability. In simple terms, increase of 33.7% (0.374–0.500) and 100.5% (0.374–0.75) in β generate the respective percent increase of PRO peak power and net electric power availability. The rapidly growing number of reported [15–25] studies on advanced TFC–PRO membrane may suggest that such membrane with $\beta \times A > 2.18$ Lmh/bar for SW–RW with power availability greater than that of MP#1 are just around the corner and should become available very soon in the near future.

The aforementioned projections (Table 2) for CC-PRO net electric power availability of 4.8–8.0 W/m^2 are in the range of clear economic feasibility for large-scale utilization especially in locations of sufficiently high quality HSF and LSF sources of minimum pretreatment requirements. The cited projections are for the CC-PRO method and if the conventional PRO method is considered instead the relevant projections are 40–55% lower.

References

[1] S. Loeb, Method and apparatus for generating power utilizing pressure-retarded-osmosis, US patent No. 3,906,250, 1975.
[2] S. Loeb, Osmotic power plants, Science 189(4203) (1975) 654–655.
[3] S. Loeb, S. Sourirajan, American chemical society advances in chemistry series, ACS 38 (1963) 117–132.
[4] A. Achilli, A.E. Childress, Pressure retarded osmosis: From the vision of Sidney Loeb to the first prototype installation—Review, Desalination 261 (2010) 205–211.

[5] B.E. Logan, M. Elimelech, Membrane-based processes for sustainable power generation using water, Nature 488 (2012) 313–319.
[6] M. Elimelech, W.A. Phillip, The future of seawater desalination: Energy, technology, and the environment, Science 333 (2011) 712–717.
[7] S. Loeb, Energy production at the Dead Sea by pressure-retarded osmosis: Challenge or chimera? Desalination 120 (1998) 247–262.
[8] S.E. Skilhagen, J.E. Dugstad, R.J. Aaberg, Osmotic power—Power production based on the osmotic pressure difference between waters with varying salt gradients, Desalination 220 (2008) 476–482.
[9] S.E. Skilhagen, G. Brekke, W.K. Nielsen, Progress in the Development of Osmotic Power, in: Proceedings Qingdao International Conference on Desalination and Water Reuse, Qingdao, China, June 20–23, 2011, pp. 247–260.
[10] G. Brekke, Review of Experience with the Statkraft Prototype Plant, in: The 3rd Osmosis Membrane Summit, Barcelona, Spain, April 26–27, 2012.
[11] A. Tanioka, Power Generation by Pressure Retarded Osmosis using Concentrated Brine from Seawater Desalination System and Treated Sewage, Review of Experience with Pilot in Japan, in: The 3rd Osmosis Membrane Summit, Barcelona, Spain, April 26–27, 2012.
[12] M. Kurihara, Government Funded Programs Worldwide, the Japanese Mega-ton Water System project, The 3rd Osmosis Membrane Summit, Barcelona, Spain, April 26–27, 2012.
[13] K. Saito, M. Irie, S. Zaitsu, H. Sakai, H. Hayashi, A. Tanioka, Power generation with salinity gradient by pressure retarded osmosis using concentrated brine from SWRO system and treated sewage as pure water, Desalin. Water Treat. 41 (2012) 114–121.
[14] A. Efraty, Closed Circuit PRO Series No 2: Performance projections for PRO membranes based on actual/ideal flux ratio of forward osmosis, Desalin. Water Treat. (2015), doi: 10.1080/19443994.2015.1010275.
[15] J.R. McCutcheon, M. Elimelech, Influence of membrane support layer hydrophobicity on water flux in osmotically driven membrane processes, J. Membr. Sci. 318 (2008) 458–466.
[16] N.Y. Yip, A. Tiraferri, W.A. Phillip, J.D. Schiffman, M. Elimelech, High Performance thin-film composite forward osmosis membrane, Environ. Sci. Technol. 44 (2010) 3812–3818.
[17] N.Y. Yip, M. Elimelech, Performance limiting effects in power generation from salinity gradients by pressure retarded osmosis, Environ. Sci. Technol. 45 (2011) 10273–10282.
[18] N.Y. Yip, A. Tiraferri, W.A. Phillip, J.D. Schiffman, L.A. Hoover, Y.C. Kim, M. Elimelech, Thin-film composite pressure retarded osmosis membranes for sustainable power generation from salinity gradients, Environ. Sci. Technol. 45 (2011) 4360–4369.
[19] N.Y. Yip, M. Elimelech, Thermodynamic and energy efficiency analysis of power generation from natural salinity gradients by pressure retarded osmosis, Environ. Sci. Technol. 46 (2012) 5230–5239.
[20] S. Chou, R. Wang, L. Shi, Q. She, C. Tang, A.G. Fane, Thin-film composite hollow fiber membranes for pressure retarded osmosis (PRO) process with high power density, J. Membr. Sci. 389 (2012) 25–33.
[21] S. Zhang, T.S. Chung, Minimizing the instant and accumulative effects of salt permeability to sustain ultrahigh osmotic power density, Environ. Sci. Technol. 47 (2013) 10085–10092.
[22] S. Zhang, F. Fu, T.S. Chung, Substrate modifications and alcohol treatment on thin film composite membranes for osmotic power, Chem. Eng. Sci. 87 (2013) 40–50.
[23] X. Li, S. Zhang, F. Fu, T.S. Chung, Deformation and reinforcement of thin-film composite (TFC) polyamide-imide (PAI) membranes for osmotic power generation, J. Membr. Sci. 434 (2013) 204–217.
[24] G. Han, S. Zhang, X. Li, T.S. Chung, High performance thin film composite pressure retarded osmosis (PRO) membranes for renewable salinity-gradient energy generation, J. Membr. Sci. 440 (2013) 108–121.
[25] X. Song, Z. Liu, D.D. Sun, Energy recovery from concentrated seawater brine by thin-film nanofiber composite pressure retarded osmosis membranes with high power density, Energy Environ. Sci. 6 (2013) 1199–1210.
[26] PCT Patent Application, Power generation by pressure retarded osmosis in closed circuit without need of energy recovery, International Publication Number WO 2012/140659 A1, 18 October 2012, inventor—Avi Efraty.
[27] A. Efraty, Closed Circuit Pressure Retarded Osmosis—A New Technology for Clean Power Generation without Need of Energy Recovery, The 3rd Osmosis Membrane Summit, Barcelona, Spain, April 26–27, 2012.
[28] A. Efraty, Pressure-retarded osmosis in closed circuit: A new technology for clean power generation without need of energy recovery, Desalin. Water Treat. 51(40–42) (2013) 7420–7430.
[29] PX: Available from: <http://energyrecovery.com/px-pressure-exchanger-energy-recovery-devices>.
[30] DWEER: Available from: <http://flowserve.com/products/energy-recovey-devices>.
[31] TOYOBO HJ-9155-PI Module and Specifications. Available from: <http://www.toyobo-global.com/seihin/ro/HB-series.htm>.
[32] A. Efraty, Closed circuit desalination series no-6: Conventional RO compared with the conceptually different new closed circuit desalination technology, Desalin. Water Treat. 41 (2012) 279–295.
[33] A. Efraty, R.N. Barak, Z. Gal, Closed circuit desalination—A new low energy high recovery technology without energy recovery, Desalin. Water Treat. 31 (2011) 95–101.
[34] A. Efraty, R.N. Barak, Z. Gal, Closed circuit desalination series no-2: New affordable technology for sea water desalination of low energy and high flux using short modules without need of energy recovery, Desalin. Water Treat 42 (2012) 189–196.
[35] A. Efraty, Closed circuit desalination series no-8: Record saving of RO energy by SWRO-CCD without need of energy recovery, Desalin. Water Treat. 52 (31–33) (2014) 5717–5730.
[36] A. Hermoni, Actual energy consumption and water cost for the SWRO systems at Palmachim—Case history, IDA conference, Huntington Beach, CA, November 2–3, 2010.